

CALCULATION METHODOLOGY FOR GEOMETRICAL CHARACTERISTICS OF THE FORMING TOOL FOR RIB COLD ROLLING

Andrej Oleinik^{1*}, Alexey Kapitanov¹, Islam Alexandrov², Aslan Tatarkanov²

¹ MSUT "STANKIN", Moscow, Russian Federation

² IDTI RAS, Moscow, Russian Federation

Calculation of the forming tool for rib cold rolling by the enveloping method is usually complex and very time-consuming. The cold rolling process is not always optimized, resulting in a poor quality of the rolled rib profile and premature failure of the forming tool. Improvement in techniques of rib rolling on metal heat-exchange tubes is a challenging technological task, which has defined the purpose of the present work – the study of the effect of the forming tool for cold rolling of ribs by enveloping method on the accuracy of geometrical dimensions of ribbed surfaces. Absence of a well-developed calculation methodology for this type of tool now adversely affects the rate of manufacturing application of rib cold rolling processes. Since the main task when introducing the rib rolling process is to achieve the required accuracy of the work-piece, it seems expedient to improve calculation methodologies allowing designing a forming tool for rib cold rolling taking into account the required accuracy of geometrical dimensions of the ribbed surfaces. The present work proposes a methodology that allows performing calculations of parameters required for manufacturing and supervision over various rolling tools. Experimental approbation data of the outlined methodology results are presented. Because of deformation processing without additional technological operations, the effect of surface hardening has been achieved, and the roughness of rolled ribbed surfaces R_a was $0.8 \mu\text{m}$, which is comparable in quality only with finishing machining. It was demonstrated that when calculating the coordinates of profile points, the geometry of the lead-in, as well as rolls with a screw rib, it is particularly important to determine the angle of crush forming rolls and the y-coordinate of rolling bars as the main characteristics of the profile.

Key words: ribbed surfaces, calculation methodology, forming tool, cold rolling, enveloping method

INTRODUCTION

Improving the quality and competitiveness of a manufacturing range, the introduction of highly productive and resource-saving technologies, and continuous scientific and technological modernization with optimal use of resources are important conditions for the economic development, as shown in works [1-3]. The technological paradigm [4] of the modern production sector is characterized by increased stock utilization ratio and the average number of operations per workplace per month according to works [5, 6]. In many respects, it is connected with a reduction of the relative role of subtractive technologies of materials processing by cutting due to the development of additive and hybrid technologies of geometry generation as well as methods of non-cutting shaping, as is proven in papers [7-9]. The use of plastic deformation methods reduces labor costs and the amount of processing waste, as demonstrated in papers [10-12]. In comparison with analogues made by cutting, products manufactured with the use of plastic deformation methods have added mechanical characteristics of surfaces, as is proven in publications [13-16] that is their competitive advantage. Common methods of metal processing nowadays are rolling, drawing, compression molding and hot and cold stamping. One of the most promising methods of plastic deformation for the formation of the

ribbed surfaces is rolling with the help of the forming tool in the form of heads with a radial arrangement of rolls driven into rotation by way of simultaneous longitudinal cold pushing of the initial workpiece [34, 35].

Possibility of the ribbed surfaces formation for heat-exchange devices can be achieved due to application of radically different technologies, as is proven in paper [17], however, the efficiency of their operation will significantly depend on the quality of surfaces. In particular, heat-exchange characteristics are significantly reduced because of clogging of the ribbed surfaces in case of their low quality, as demonstrated in publications [18-20]. The roughness of ribbed heat exchange surfaces has a significant impact on the efficiency of their operation. With its high productivity, the rolling technique ensures high quality of the ribbed surface due to improving its smoothness and simultaneous hardening, as shown in paper [21].

Nevertheless, the industrial introduction of the cold rolling method is fraught with certain difficulties. Since the cold rolling process is not always optimized according to papers [22-26], in practice premature destruction of the rolling tool in case of the low accuracy of the rolled rib profile is often observed, as is proven by the authors of papers [27, 28]. As can be seen from the above, the improvement of the rib rolling forming technology on metal

* olejnikandrejv@yandex.ru

heat-exchange tubes is a challenging technological task which has defined the purpose of the present work that was to study the effect of the forming tool for cold rolling of ribs by way of enveloping on the accuracy of geometrical dimensions of the ribbed surfaces.

LITERATURE REVIEW

For the formation of the ribbed surfaces, various technological methods can be applied; however, the choice of one or another technology is defined not only by design features of a manufactured product but also by economic feasibility and productivity. In most cases, the manufacturing cost of technological operations of ribbed surfaces forming by cold rolling method turns out to be much lower in comparison with cutting processing, as shown in paper [10]. The reason for this is higher productivity of the method, a higher utilization factor of the processed material, lower costs for depreciation of equipment and replacement of machining tools as disclosed in work [29]. Besides, cold plastic processing has a number of technical advantages in comparison with other forming methods, the main of which are low roughness and hardening of the part surface (Table 1).

Under pressure, which exceeds the value of the flow stress of the processed material as a condition shown in paper [10], plastic deformation occurs in the material at room temperature, as demonstrated in work [13], the result of which is not only the formation but also a significant change in material characterization of the processed part, as is proved in paper [15]. Rolling is accompanied by an intensive increase in the surface hardness of the part and hardening of its material, as shown in paper [16]. Wear resistance of products manufactured by plastic deformation is 30-40 % over than of milled ones, and strength characteristics of rolled ribs are up by 10-20 %. The change in properties of the strained material is connected with changes in its structure, occurring at various scale levels under the action of technological processing conditions according to the Curie principle, as stated in papers [30-32]. Besides the change of the

processed material properties under the action of the smooth and practically non-deformable tool, the roughness of the processed surface decreases according to work [21]. In addition to it, an important advantage of the rib rolling method is a high dimensional stability of the machining tool as indicated by the authors of paper [28], which is maintained at the level of the original one during the whole running time of the tool.

Although the listed forming processes and changes in the structure and properties of the material happen simultaneously, they have different intensity and, therefore, the resulting cold rolling effect can be significantly different. Depending on the required effect of processing, it is necessary to choose the appropriate technological modes for each particular pair of the forming tool and processed product taking into account the applied equipment and the type of the technological operation. Usually, the main task when introducing the rib rolling process is to achieve the required accuracy of the workpiece. Besides the experimental approach for the solution of this problem, it is expedient to apply the calculation methodologies allowing designing a forming tool for cold rolling of ribs taking into account the required accuracy of the ribbed surfaces. Since the accuracy is characterized not only by the accuracy of geometric dimensions but also by the accuracy of the shape and mutual location as well as by roughness of surfaces, special attention has been given to these particular parameters in the article.

METHODOLOGY

The deformation processing method is one of the most significant factors determining the design of the machining tool. The kinematic process of rolling of the line profile ribs by enveloping method is similar to the process of rib manufacturing by slotting or milling [33]. The difference consists only in a few working motions typical for each machining method. The basis for obtaining a theoretically correct tool profile is the principle of mutual enveloping of the triangular rib profile and the tool when rolling the centre of the triangular rib profile over the

Table 1: Comparison of methods for ribbed surfaces forming of parts

| Characteristics | Powder metallurgy, including surfacing | Casting | Mechanical processing | Cold rolling |
|---------------------------------------|--|---------------|-----------------------|---------------|
| Range of wall thicknesses, mm | More than 2 | More than 5 | More than 0.1 | More than 0.1 |
| Proportion of theoretical density, % | 85-90 | 94-99 | 100 | 100 |
| Proportion of theoretical strength, % | 75-85 | 94-97 | 100 | 100 and more |
| Typical part surface roughness Ra, μm | More than 2 | More than 3 | 0.4-2 | 0.8-1.6 |
| Effective production volume, pcs. | More than 500 | More than 500 | More than 1 | More than 1 |

centrode of the tool without sliding. The following theoretical provisions must be implemented for cold rolling of ribs by enveloping method:

- Conjugated profiles must have a common contact tangent and normal;
- The normal drawn through the contact point of the conjugated profiles must pass through the profiling pole, which is the tangential point of the tool and the centrodes of the triangular rib profile.
- Depending on the nature of the working motions during rolling, the forming tool can be classified as follows:
- A tool with a radius of the finite quantity centrode that performs a rotational motion during rolling (rollers, roller heads, etc.);
- A tool with infinite radius centrode, having a straight-line direction of the main motion (flat bars, round cross-section bars).

The calculation methodology of the forming tool for rolling of the line profile ribs presented in this paper is composed of three independent stages. At the first stage, the calculations related to the manufacturing of the rolling tool are performed. These include:

- Initial parameters selection of the reference profile of the triangular ribs;
 - Calculation of the pitch circle radius of the triangular rib profile;
 - Calculation of the workpiece diameter;
 - Calculation of basic geometrical parameters of the tool.
1. To achieve the required accuracy of the ribbed surface, the calculation of the rolling tool should be based on the reference rib profile with adjusted dimensions. The adjustment shall be carried out, taking into account the elastic recovery of the workpiece metal by expression (1):

$$\Delta d_{cp} = \frac{\sigma_B}{E} d_{cp} \quad (1)$$

where Δd_{cp} is the value of the absolute change of the rib profile average diameter, σ_B is the ultimate tensile strength of the workpiece material, E is the modulus of elasticity of the workpiece material, d_{cp} is the average diameter of the rib profile.

The choice of geometrical elements of the profile (Figure 1) is carried out according to the formulas:

$$d_e = d_{ch} - \left(\frac{1}{2} \div \frac{2}{3}\right) \delta_e; \quad d_1 = d_{1H} - \left(\frac{1}{2} \div \frac{2}{3}\right) \delta_1; \quad (2)$$

$$d_2 = d_{2H} - \left(\frac{1}{2} \div \frac{2}{3}\right) \delta_2$$

in which d_e is the outer average diameter of the manufactured product; d_{ch} is the outer average diameter of the crush forming roll; δ_e is the tolerance range of the average diameter; d_1 is the diameter of the manufactured product rib in its top point; d_{1H} is the diameter of the crush

forming roll in its lower point; δ_1 is the diameter tolerance range in the rib top of the crush forming roll; d_2 is the diameter of the manufactured product rib in its lower point; d_{2H} is the diameter of the manufactured product rib in its lower point; d_{2H} is the diameter of the crush forming roll in its top point; δ_2 is the diameter tolerance range in the lower point of the rib.

After that, the constant parameter of the triangular ribs profile e is calculated. All notations are shown graphically in Figures 2 and 3. For straight-sided ribs, the profile parameter e corresponds to the expression (3a):

$$e = \frac{b}{2} \quad (3a)$$

where b is the width of the straight-sided rib. For the ribs of the triangular profile, parameter e is found from the expression (3b):

$$e = r_1 \sin \frac{\beta}{2} \quad (3b)$$

in which β is the pressure angle at the top of the rib; r_1 is the radius of the addendum circle along the full profile; r is the radius of the pitch circle of the profile.

Tool wear during the rolling process and thermal deformations are not taken into account in the calculation, because they are so small that practically have no impact on the accuracy of the rolled products.

2. When calculating the minimum possible radius of the pitch circle of the triangular rib profile, the formula (4a) is used for the crush forming rolls and formula (4b) is used for the rolling bars. The following notations are used in the formulas: γ is the pressure angle of the triangular ribs; r_e is the radius of the addendum circle. These formulas define the possibility of processing the tool profile to its full height.

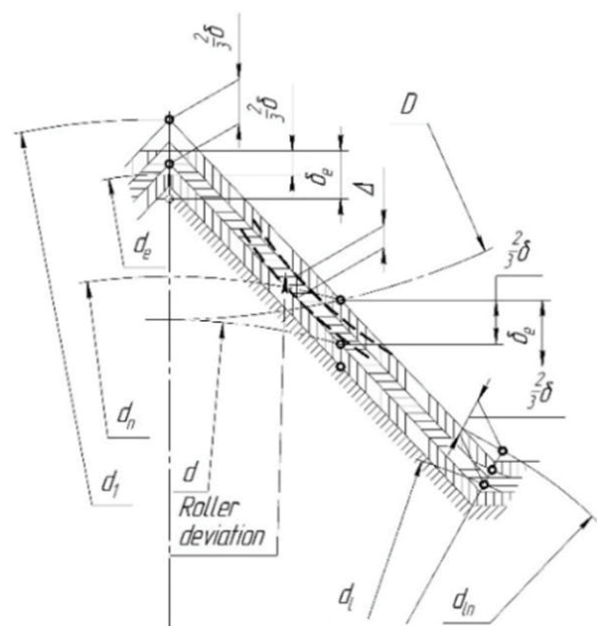


Figure 1: Tolerance range distribution of the crush forming roll and triangular ribs profile

$$r_{\min} = \sqrt{r_e^2 - \frac{2i+3}{(2i)^2} \sin \gamma} \quad (4a)$$

$$r_{\min} = \sqrt{r_e^2 + \frac{3}{4} e^2} \quad (4b)$$

The radius of the pitch circle of the rib profile r is taken as close as possible to the calculated value of the workpiece radius in the range from r_{\min} to r_e , which ensures the correct division of the workpiece by the required number of ribs because the circular pitches of the conjugated profiles have the same value only on the pitch circles.

3. The preliminary calculation of the workpiece diameter is carried out from the condition of equality of areas of cross-sections of the workpiece and the finished part and subsequently is defined more precisely on the basis of experimental data.
4. The calculation of the gearing characteristics (Figures 2 and 3) includes:
 - The determination of the circular pitch t_0 by the for-

mula (5a), in which z is the number of rolling ribs:

$$t_0 = \frac{2\pi r}{z} \quad (5a)$$

- The determination of the gearing ratio i by the formula (5b), in which z_p is the number of ribs on the roll:

$$i = \frac{z}{z_p} \quad (5b)$$

- The determination of the centre-to-centre distance A by the formula (5c), in which R is the radius of the pitch circle of the rolling tool:

$$A = R + r \quad (5c)$$

5. Basic geometrical parameters of the rolling tool (Figures 2 and 3) are calculated for the crush forming rolls according to the following formulas:

- The number of ribs on the crush-forming roll z_p is rounded to an integer value based on the approximate radius of the crush forming roll R_{CP} :

$$Z = \frac{zR_{CP}}{r_e} \quad (6a)$$

- The radius of the pitch circle of the rolling tool R :

$$R = \frac{r}{i} \quad (6b)$$

- The radius of the addendum circle of the rolling tool R_e :

$$R_e = A - r_e \quad (6c)$$

- The radius of the dedendum circle of the rolling tool R_i :

$$R_i = A - r_i \quad (6d)$$

- The rib height h based on the radius of the lower point of the rib r_i when rolling:

$$h = r_e - r_i \quad (6e)$$

Then the calculation of additional parameters necessary for the complete control of the tool is performed, more

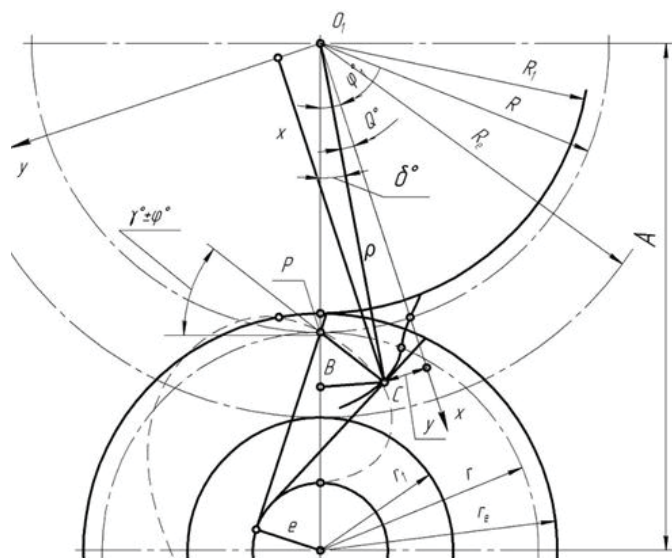


Figure 2: Point coordinates plotting of the crush forming roll profile

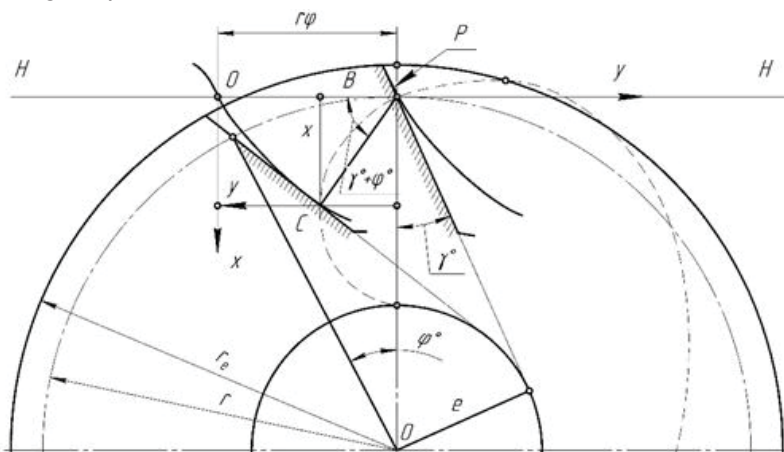


Figure 3: Point coordinates plotting of the rolling bar profile

specifically: 1) calculation of coordinates of profile points (x, y); 2) calculation the diameter d_p of the control crush forming roll.

The curve of the working tool profile, obtained because of profiling by the enveloping method, is complex and therefore is usually described by equations in parametric form. One of the following geometric elements may serve as a parameter in the derivation of these equations: the current rotation angle, triangular rib profile φ ; variable radius of the triangular rib profile ρ_{un} or tool profile ρ .

In this case, the variable parameter for the crush forming rolls is the current tool radius ρ , and for the rolling bars – the x-coordinate. The procedure for the calculation of the profile point coordinates is as follows.

1. For the crush forming rolls: 1) the current rotational angle φ is calculated; 2) the auxiliary angle δ (the vertical contact angle when rolling by the crush forming rolls) is calculated; 3) the pressure angle θ is determined; 4) coordinates x, y of the profile points are calculated.
2. For the rolling bars: 1) the determination of the current rotational angle φ ; 2) the calculation of the y-coordinate of the profile.

Formulas for calculating the point coordinates of the crush forming roll profile are derived in a rectangular coordinate system associated with the roll profile (see Fig. 2) and originating at the point O_1 , which is the center of the roll. By taking an arbitrary radius value ρ within the range from R_1 to R_e , which corresponds to some rotational angle of the triangular ribs profile φ and the tool profile $\varphi_1 = \varphi$, equality is written from the rectangular triangle BO_1C :

$$O_1C^2 = O_1B^2 + BC^2 \quad (7)$$

in which each of the summands is defined by the following expressions:

$$O_1B = R + PC \sin(\gamma \pm \varphi) \quad (8)$$

$$O_1C = PC \sin(\gamma \pm \varphi)$$

where PC is the common normal line of the conjugate profiles:

$$PC = r [\sin(\gamma \pm \varphi) - \sin \gamma] \quad (9)$$

Substituting the found values into the equality (7) and solving the resulting square equation for $\sin(\gamma \pm \varphi)$, we obtain the expression (10):

$$\sin(\gamma \pm \varphi) = (1+i) \frac{\sin \gamma}{(2+i)} + \sqrt{\left(\frac{\sin \gamma}{2+i}\right)^2 + \frac{k^2 - 1}{i(2+i)}} \quad (10)$$

in which the ratio ρ/R is expressed by the coefficient k.

From the same triangle BO_1C let us define $\sin(\delta)$:

$$\sin \delta = \frac{BC}{O_1C} = \frac{r}{\rho} [\sin(\gamma \pm \varphi) - \sin \gamma] \cos(\gamma \pm \varphi) \quad (11)$$

The pressure angle represents the following difference:

$$\Theta = \varphi_1 - \delta = [(\gamma \pm \varphi) - \gamma]i - \arcsin \left\{ \frac{i}{k} [\sin(\gamma \pm \varphi) - \sin \gamma] \cos(\gamma \pm \varphi) \right\} \quad (12)$$

The coordinates of the profile points are determined by the system of equations (13):

$$\begin{cases} x = \rho \cos \Theta \\ y = \rho \sin \Theta \end{cases} \quad (13)$$

After calculating the pressure angle θ , it is necessary to check the overlap of the angle θ_{max} . Because of the wrong choice of the pitch circle radius of the crush forming roll $R = r/i$, the pressure angle θ may take a value higher than the maximum permissible θ_{max} , which may lead to underestimating of the profile height during the machining process. Therefore, the condition of $\theta \leq \theta_{max}$ must be followed, which, taking into account that $\theta_{max} = (\delta_t - \delta_s)/2$ will take the following form (14):

$$\Theta \leq \frac{\delta_t - \delta_s}{2} \quad (14)$$

where δ_t is the angular pitch of the roll; δ_s is the central angle corresponding to the width of the space along the arc of the pitch line.

If this condition is not met, the value of the radius R should be increased by reducing the radius of the pitch circle of the triangular rib profile r.

In deriving the formulas for calculating the coordinates of the profile points (x, y) of the rolling bars, the variable parameter is the x-coordinate of the point C, which belongs to the rib profile and the bar profile simultaneously, rotated relative to the initial position, shifted from the point P by a distance $PO = r\varphi$ (see Figure 3). In this case, the rectangular coordinate system O_{xy} with the beginning at the intersection of the bar profile with the initial line is built so that the O_x axis passes through the profile centre of the triangular ribs and the O_y axis coincides with the initial line of the bar.

From the triangle PCB we will obtain the expression (15):

$$PC \cos(\gamma \pm \varphi) = \frac{x}{\operatorname{tg}(\gamma \pm \varphi)} \quad (15)$$

By substituting PC from the equality (9), as well as by transforming and moving the entire numerical expression to the left side, we can obtain a square equation (16):

$$r \sin^2(\gamma \pm \varphi) - r \sin \gamma \sin(\gamma \pm \varphi) - x = 0 \quad (16)$$

The solution of the equation (16) is the expression (17) defining the angle φ as a function of the x-coordinate:

$$\sin(\gamma \pm \varphi) = \frac{\sin \gamma}{2} + \sqrt{\left(\frac{\sin \gamma}{2}\right)^2 + k_1} \quad (17)$$

where k_1 is a variable equal to x/r .

The y-coordinate is defined by the following expression:

$$y = r [(\gamma \pm \varphi) - \gamma - (\sin(\gamma \pm \varphi) - \sin \gamma) \cos(\gamma \pm \varphi)] \quad (18)$$

From the presented analytical dependencies, it follows that the most important in terms of the required accuracy of the calculation are formulas for determining the minimum radius of the pitch circle of the profile of the triangular ribs r_{\min} and the pressure angle of the crush forming rolls (or y-coordinates of the rolling bars).

At the third stage, the calculation of geometrical parameters of the lead-in of the crush forming rolls, working according to the scheme with the axial feed of the workpiece, is performed. The calculation reduces to determining the length of the lead-in m_1 and the vertex angle α_1 depending on the given values of the cone angle α .

The ribs of the crush forming rolls can have a straight-line or curved profile, which geometry is determined by the geometry of the cutting tool and the method of profiling. The most expedient for economical energy consumption in metal deformation in the process of rib formation during rolling should be considered a profile limited by a curve, which by nature close to the profile curve of the calibration part of the rolls. Under this condition, at the transition from the lead-in to the calibrating part, the minimum energy is spent for the secondary metal deformation associated with the final formation of the profile of the triangular ribs with the help of the calibrating part of the rolls. This profile can be obtained, for example, by machining with a shaping cutter using the enveloping method.

Let the process of profile cutting of the calibration and lead-in parts be performed with a tool whose profile corresponds to the reference rib profile. As the cone serves as a poloidal surface, when cutting the ribs of the lead-in, with a constant gear ratio i and a constant angular pitch δ_i the circular pitch t_0 has a variable value along the length of the lead-in $t_0 \neq t_0'$, and the width of the space along the arc of the pitch circle has the same values at any point of the poloidal cone. Therefore, the circular pitch t_0 is reduced by reducing the thickness of the roll rib. At the same time, the profile height is reduced, and at the point C (C') the profile height is the same as the height of its foot.

Then let us take the normal section I-I, passing through the point A, and the section II-II, crossing the polhode in the point B. We will project the rib profiles obtained in these sections onto the common plane parallel to the two secants. The circular steps t_0 and t_0' will be equal to their values taken on the elevation, and the radii of the pitch circles in these sections, representing the distances R_{np} and R'_{np} from the considered points A and B to the actual axis of rotation of the roll, will have a variable value, which is determined by the formulas:

$$R_{\text{np}} = \frac{R}{\cos \alpha} \quad R'_{\text{np}} = \frac{R'}{\cos \alpha} \quad (19)$$

The reduced gearing ratio is also different from the actual ratio (20):

$$i_{\text{TP}} = \frac{r}{R_{\text{TP}}} = i \cos \alpha \quad i'_{\text{TP}} = \frac{r}{R'_{\text{TP}}} \quad (20)$$

The pressure angle θ is equal to the difference of angles (21):

$$\Theta_1 = \frac{1}{2}(\delta_{t1} - \delta_s) \quad \Theta_2 = \frac{1}{2}(\delta_{t2} - \delta_s) \quad (21)$$

Knowing the pressure angle of the triangular ribs γ , the pressure angle of the roll from θ_1 and θ_2 as well as the reduced values of the gearing ratios i_{np} and i'_{np} , we will find the values of radii of the addendum circles along the full profile in these sections R_1 and R'_1 .

The taper lead-in actual angle α_1 is determined by the expression (22):

$$\alpha_1 = \alpha + \beta_1 \quad (22)$$

We will find the taper lead-in projection angle β_1 by expression (23) from the ACA_1 triangle:

$$\tan \beta_1 = \frac{AA_1}{CA} \quad (23)$$

A segment of CA is defined by the expression (24) from the ACD triangle:

$$CA = \frac{AD}{\sin \alpha} \quad (24)$$

The full profile height AA' in the section I-I is defined by expression (25):

$$AA' = R_1 - \frac{R}{\cos \alpha} \quad (25)$$

By substituting dependencies (23)-(25) into the expression (22), we will get the dependence (26):

$$\alpha_1 = \alpha + \arctg \left[\frac{2\pi}{z_p} \operatorname{tg} \alpha \left(\frac{R_1 \cos \alpha - R}{t_0 - \frac{2\pi r}{z_p}} \right) \right] \quad (26)$$

We will define the length of the lead-in m_1 from the triangle A_1EK by the expression (27), and the segment BE will be found by the formula (28):

$$m_1 = \frac{KE}{\operatorname{tg} \alpha_1} = \frac{R_e - R + a - BE}{\operatorname{tg} \alpha_1} \quad (27)$$

$$BE = BE_1 + E_1E = BB_1 \frac{(\cos \alpha_1 + \sin \alpha \sin \beta_1)}{\cos \alpha \cos \alpha_1} \quad (28)$$

By substituting the value of BE from the formula (28) into the expression (27) and identically transforming the formula (27), we will determine m_1 by the formula (29):

$$m_1 = \frac{(R_e - R + a) \cos^2 \alpha \cos \alpha_1 - (R'_1 \cos \alpha - R + a) (\cos \alpha_1 + \sin \alpha \sin \beta_1)}{\sin \alpha_1 \cos^2 \alpha} \quad (29)$$

It should be noted that the rib profiles in normal I-I and end III-III sections have different geometrical parameters. In particular, the curvature of their side surface depends on the pressure angle γ of the rolling tool. The correlation between the actual angle γ in the normal cross-section and its projection γ_1 in the end section is determined by the equality (30):

$$\operatorname{tg} \gamma_1 = \operatorname{tg} \gamma \cos \alpha \quad (30)$$

As can be seen from the above, it was demonstrated that it is possible to change the geometry of the lead-in profile and bring it closer to the profile geometry of the calibration part by changing the pressure angle of the tool making the lead-in profile.

RESULTS AND DISCUSSION

Experimental testing of the calculation results gained according to the presented methodology was carried out. Rolling was performed on a vertical milling machine in a three-rolls rolling device with feed-out of the workpiece. Test results of the rolled products demonstrated that the un straightness of the rib profile in the normal section did not exceed 0.008 mm and the variation in a dimension of the rolls did not exceed 0.04 mm; the tangential pitch error was ± 0.015 mm. Because of deformation processing without additional technological operations, the effect of surface hardening has been achieved, and the roughness of the rolled ribbed surfaces R_a was $0.8 \mu\text{m}$, which is comparable in quality only with finishing machining.

Besides, it was found that the use of machining tools with the pitch or gradient of working coils error leads to the formation of surface defects such as "fold" regardless of the contour filling degree. As well, surface defects such as folds, layers and burrs (Figure 4) as well as defects in the form of metal pitting and cracking may also take place.

The main reason for the formation of defects during the rolling process is related to the conditions of rib profiling. Swelling of the profile takes place due to the redistribution of elementary volumes of metal, displaced by the working coils of the forming tool. In the process of the profile swelling, it appears that the emergence of both symmetrical and asymmetrical deformation is possible. The nature of the deformation depends on the way that working windings of the rolling tool pass over the surface of the forming rib, i.e. the windings either coincide or not. The formation of defects at the tip of the full rib profile is possible due to symmetrical deformation. However, the defects in the rib profile may have a different arrangement depending on the displacement value of the tool profile in the deformation cycle. Adjustment of the rolling machine when the butt beat tool installation also leads to asymmetry of the metal deformation, with the conse-

quence that the paths of the tool windings do not match and defects take place in the form of folds, layers and rolling laps, etc. Breaking the symmetry of metal deformation during cold rolling of the ribs mainly takes place in the following cases:

- because of the wrong displacement of the forming tool;
- because of the poor quality of the machining tools;
- because of the complete filling of the winding profile during rolling;
- because of the low rigidity of the rolling machine used.

The main types of destruction of the rolling tool are irreversible deformations and fire cracking. Until the present time, there has not been formed a simple and unified theoretical apparatus describing the influence of aggregate factors on the destruction of the tool during its manufacture and operation. Nevertheless, the most important factors that determine the durability of a forming tool can be divided into design and operational ones. The design factors are the geometry of the tool, chemical composition of its material, type of heat treatment, hereditary technological features of the production of the tool itself, etc. Operational factors include the deformation method, temperature and degree of deformation as well as the type of lubrication. Furthermore, subjective factors should also be mentioned, such as skills of workers and their compliance with technological instructions, and production culture in general. The variety of factors acting in the process of the forming tool operation and the lack of sufficient amount of accumulated experimental data on the working conditions of the tool in many respects complicate the possibility of the theoretical analysis and development of new solutions to improve the quality of the forming tool.

CONCLUSIONS

Manufacturing application of cold rolling of the rib profiles leads to the significant increase in productivity and quantity reduction in processing waste. The present work proposes a methodology that allows you to perform calculations of parameters required for manufacturing and supervision over various rolling tools. Experimental approbation data of the outlined methodology results are presented. It was demonstrated that determining the angle of the crush forming rolls and y-coordinates of the rolling bars as the main characteristics of the profile is of particular importance for the calculation of the rolling tool profile. The worked-out technological process has high productivity, and the obtained products at low roughness have high mechanical properties of the formed surfaces. Because of deformation processing without additional technological operations, the effect of surface hardening has been achieved, and the roughness of the rolled ribbed surfaces R_a was $0.8 \mu\text{m}$, which is comparable in quality only with finishing machining.

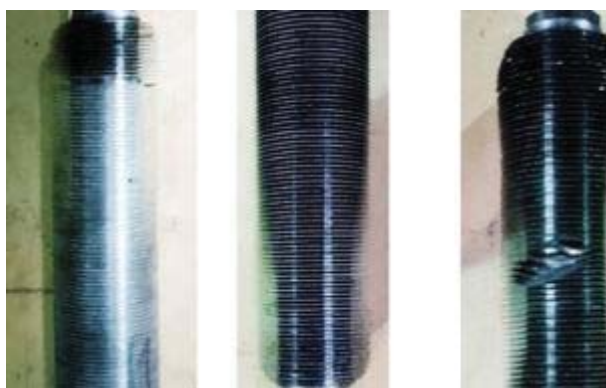


Figure 4: Defects in rib rolling

ACKNOWLEDGEMENTS

Some results of this manuscript were obtained as a part of the work under the Agreement on the provision of subsidies under date of 13 December 2019 No. 75-15-2019-1941 (the agreement internal number 05.607.21.0321) on the topic: "Development of design and technological solutions for modular pre-fabricated transmission line towers with integrated systems for continuous digital monitoring of the condition and thermal stabilization of the soil to meet the needs of the Arctic regions and the Far North" with the Ministry of Science and Higher Education of the Russian Federation. The unique identifier of the applied research (project) is RFMEFI60719X0321.

REFERENCES

1. Hakansson, H. (2015). *Industrial Technological Development*. Routledge Revivals, London. doi:10.4324/9781315724935.
2. Acemoglu, D. (2012). Introduction to economic growth. *Journal of Economic Theory*, vol. 147, no. 2, 545–550. doi:10.1016/j.jet.2012.01.023.
3. Olejnik, A.V. (2009). The tasks of intellectual development and support of innovative infrastructure in the Russian Federation. *Scientific and Technical Information Processing*, vol. 36, pp. 1, 39–42. doi:10.3103/s0147688209010055.
4. Glazyev, S. (2018). Discovery of Regularities of Changes of Technological Orders in the Central Economic and Mathematics Institute of the Soviet Academy of Sciences. *Economics and Mathematical Methods*, vol. 3, 17–30. doi:10.31857/s042473880000655-9.
5. Hitomi, K. (2017). *Manufacturing Systems Engineering*. Routledge, London. doi:10.1201/9780203748145.
6. Agafonov, F., Genin, A., Kalinina, O., Brel, O., Zhironkina, O. (2017). Technological convergence and innovative development of natural resource economy. *E3S Web of Conferences*, vol. 15, 04011. doi:10.1051/e3sconf/20171504011.
7. Zheng, D. (2015). *Industrial Engineering and Manufacturing Technology*. Proceedings of the 2014 International Conference on Industrial Engineering and Manufacturing Technology (ICIEMT 2014), July 10–11, 2014, Shanghai, China. doi:10.1201/b18144.
8. Semenov, A.B., Fomina, O.N., Muranov, A.N., Kutsbakh, A.A., Semenov, B.I. (2019). The Modern Market of Blank Productions in Mechanical Engineering and the Problem of Standardization of New Materials and Technological Processes. *Advanced Materials & Technologies*, vol. 1, 003–011. doi:10.17277/amt.2019.01.pp.003-011.
9. Semenov, A.B., Kutsbakh, A.A., Muranov, A.N., Semenov, B.I. (2019). Metallurgy of thixotropic materials: the experience of organizing the processing of structural materials in engineering Thixo and MIM methods. *IOP Conference Series: Materials Science and Engineering*, vol. 683, 012056. doi:10.1088/1757-899x/683/1/012056.
10. Jiang, Z.Y. (2011). *Mechanics of cold rolling of thin strip. Numerical analysis—Theory and application*, InTech Open, Rijeka, 439–462. doi:10.5772/23344.
11. Gubanova, N.V., Karelin, F.R., Choporov, V.F., Yusupov, V.S. (2011). Study of rolling in helical rolls by mathematical simulation with the DEFORM 3D software package. *Russian Metallurgy (Metally)*, vol. 2011, no. 3, 188–193. doi:10.1134/s0036029511030074.
12. Fedorov, S.V., Aleshin, S.V., Swe, M.H., Abdirova, R.D., Kapitanov, A.V., Egorov, S.B. (2017). Comprehensive surface treatment of high-speed steel tool. *Mechanics & Industry*, vol. 18, no. 7, 711. doi:10.1051/meca/2017066.
13. Johnson, K.L. (2000). Plastic Deformation in Rolling Contact. *Rolling Contact Phenomena*, 163–201. doi:10.1007/978-3-7091-2782-7_3.
14. Bower, A.F., Johnson, K.L. (1989). The influence of strain hardening on cumulative plastic deformation in rolling and sliding line contact. *Journal of the Mechanics and Physics of Solids*, vol. 37, no. 4, 471–493. doi:10.1016/0022-5096(89)90025-2.
15. Mc Dowell, D.L., Moyar, G.J. (1990). Effects of non-linear kinematic hardening on plastic deformation and residual stresses in rolling line contact. *Mechanics and Fatigue in Wheel/Rail Contact*, 19–37. doi:10.1016/b978-0-444-88774-0.50006-7.
16. Yoshimi, T., Matsumoto, S., Tozaki, Y., Yoshida, T., Sonobe, H., Nishide, T. (2009). Work Hardening and Change in Contact Condition of Rolling Contact Surface with Plastic Deformation. *Tribology Online*, vol. 4, no. 1, 1–5. doi:10.2474/trol.4.1.
17. Wais, P. (2012). *Fin-Tube Heat Exchanger Optimization*. Heat Exchangers - Basics Design Applications. InTech, Rijeka. doi:10.5772/33492.
18. Wang, F., Liang, C., Yang, M., Fan, C., Zhang, X. (2015). Effects of surface characteristic on frosting and defrosting behaviors of fin-tube heat exchangers. *Applied Thermal Engineering*, vol. 75, 1126–1132. doi:10.1016/j.applthermaleng.2014.10.090.
19. Carija, Z., Frankovic, B., Percic, M., Cavrak, M. (2014). Heat transfer analysis of fin-and-tube heat exchangers with flat and louvered fin geometries. *International Journal of Refrigeration*, vol. 45, 160–167. doi:10.1016/j.ijrefrig.2014.05.026.

20. Kim, K., Lee, K.-S. (2013). Frosting and defrosting characteristics of surface-treated louvered-fin heat exchangers: Effects of fin pitch and experimental conditions. *International Journal of Heat and Mass Transfer*, vol. 60, 505–511. doi:10.1016/j.ijheatmasstransfer.2013.01.036.
21. Li, Z. (2018). Elastic Deformation of Surface Topography under Line Contact and Sliding-rolling Conditions. *Journal of Mechanical Engineering*, vol. 54, no. 5, 142. doi:10.3901/jme.2018.05.142.
22. Jiang, Z., Xie, H. (2018). Application of Finite Element Analysis in Multiscale Metal Forming Process. *Finite Element Method - Simulation, Numerical Analysis and Solution Techniques*. InTech, Rijeka. doi:10.5772/intechopen.71880.
23. Hong-Seok Park, Tran Viet, Anh. (2010). Finite Element Analysis of roll forming process of aluminum automotive component. *International Forum on Strategic Technology 2010*. doi:10.1109/ifost.2010.5667921.
24. Hao, L., Jiang, Z., Wei, D., & Chen, X. (2013). Finite element analysis of roll bit behaviors in cold foil rolling process. *AIP Conference Proceedings*, vol. 1532, 478. doi:10.1063/1.4806864.
25. Jung, D.W. (2018). Finite Element Analysis for the Roll Forming Process of Rib. *Applied Mechanics and Materials*, vol. 878, 302–307. doi:10.4028/www.scientific.net/amm.878.302.
26. Tsang, K.S., Ion, W., Blackwell, P., English, M. (2017). Validation of a finite element model of the cold roll forming process on the basis of 3D geometric accuracy. *Procedia Engineering*, vol. 207, 1278–1283. doi:10.1016/j.proeng.2017.10.883.
27. Strycharska, D., Szota, P., Mroz, S. (2017). Increasing the Durability of Separating Rolls during Rolling Ribbed Bars in the Three-Strand Technology. *Archives of Metallurgy and Materials*, vol. 62, no. 3, 1535–1540. doi:10.1515/amm-2017-0236.
28. Szota, P., Strycharska, D., Mroz, S., Stefanik, A. (2015). Analysis of Rolls Wear during the Ribbed Bars Multi-Slit Rolling Process. *Archives of Metallurgy and Materials*, vol. 60, no. 2, 815–820. doi:10.1515/amm-2015-0212.
29. Strycharska, D. (2019). Analysis of Roll Wear Costs During Multi-Strand Rolling of Ribbed Bars Using New Slitting Pass System. *New Trends in Production Engineering*, vol. 2, no. 2, 267–278. doi:10.2478/ntp-2019-0091.
30. Karkina, L.E., Zubkova, T.A., Yakovleva, I.L. (2013). Dislocation structure of cementite in granular pearlite after cold plastic deformation. *The Physics of Metals and Metallography*, vol. 114, no. 3, 234–241. doi:10.1134/s0031918x13030095.
31. Yakovleva, I.L., Karkina, L.E., Zubkova, T.A., Tabat-chikova, T.I. (2011). Effect of cold plastic deformation on the structure of granular pearlite in carbon steels. *The Physics of Metals and Metallography*, vol. 112, no. 1, 101–108. doi:10.1134/s0031918x11010388.
32. Qiao, X.G., Gao, N., Starink, M.J. (2012). A model of grain refinement and strengthening of Al alloys due to cold severe plastic deformation. *Philosophical Magazine*, vol. 92, no. 4, 446–470. doi:10.1080/14786435.2011.616865.
33. Luo, W., Chen, Y., & Zhang, G. (2015). Helix error testing and tracing on planar enveloping hourglass worm tooth surface. *Xinan Jiaotong Daxue Xuebao/Journal of Southwest Jiaotong University*, 50(2), 279–285. doi:10.3969/j.issn.0258-2724.2015.02.011
34. Wei, X., & Jiang, S. (2017). Fatigue life prediction on rib-to-deck welded joints of steel bridge deck based on LEFM. *Xinan Jiaotong Daxue Xuebao/Journal of Southwest Jiaotong University*, 52(1), 16–22. doi:10.3969/j.issn.0258-2724.2017.01.003
35. Antufiev, B.A., Egorova, O.V., Orekhov, A.A., Kuznetsova, E.L. (2018). Dynamics of a Clamped Ribbed Plate under Moving Loads. *Periodico Tche Quimica*, vol. 15, special issue 1, 368–376.

Paper submitted: 13.02.2020.

Paper accepted: 31.03.2020.

This is an open access article distributed under the CC BY-NC-ND 4.0 terms and conditions.